Design and Experimental Testing of Holly Pruning Machine with Adaptive Adjustment Tool

Xiuhao Yu , Chengming Hou, Liqi Qiu , Xuesong Li, Penghui Yao, and Ying Zhao , *

To improve the efficiency of holly pruning, effectively solve the labor intensity of manual handheld pruning machines, and the frequent replacement of tools when pruning different shapes of hollies, this study designed a pruning machine with adaptive tool adjustment. A combination of theoretical calculations, fluid dynamics simulation and analysis, and field testing was employed to design spray application mechanisms and verify their feasibility. Visual distance measurement and target recognition algorithms were used to design visual mechanisms, which were experimentally validated. Based on the principles of kinematics and dynamic simulation analysis, adaptive tool adjustment mechanisms were designed, and the key factors influencing the pruning smoothness rate and residual branch rate of the pruning equipment were identified. Based on the force analysis and parameters from the experimental results, the machine performed well, with a cutting mechanism motor speed of 20.9 kr/min, a tool tilt angle of 50°, and a walking speed of 0.91 m/s. The machine achieved a pruning smoothness rate of 79.3% and a residual branch rate of 8.1%, thereby meeting the requirements for holly pruning in horticultural operations.

DOI: 10.15376/biores.20.3.6736-6764

Keywords: Holly; Holly pruning; Adaptive tool adjustment; Spraying; Vision

Contact information: School of Mechanical and Automotive Engineering, Liaocheng University, Liaocheng 252059, China; *Corresponding author: zhaoying@lcu.edu.cn

INTRODUCTION

Ilex (holly) is the largest dioecious plant genus in the holly family (Aquifoliaceae) and occurs in tropical and temperate regions (Chong et al. 2023; Zhou et al. 2023, 2024). Holly remains green in all seasons (Christenhusz et al. 2024) and has strong tolerance to waterlogging (Zhou et al. 2023). Holly originated in southeastern China (Peng et al. 2016) and is widely distributed throughout China. It has a strong ability to adapt to different environments. Its root system has a strong adsorption capacity for heavy metals in the soil (Prasad and Freitas 2000), which is conducive to reducing heavy metal pollution in the environment. Holly possesses unique ornamental value (Feng et al. 2023), high adaptability to the environment, and purification of heavy metal pollution, and it is often used as an ornamental and greening plant in gardens (Su et al. 2020; Guo et al. 2023; Chen et al. 2024). Regular pruning, as an important technical measure in holly cultivation, promotes morphological regulation and physiological growth (Gokavi et al. 2021). However, the current manual pruning model has significant efficiency bottlenecks, incurring high human resource costs while maintaining the plant shape. The currently used pruning machine for holly trimming in China is dominated by hand-held hedge trimmers,

which have the disadvantage of consuming a large amount of labor, high cost, and low efficiency (Li *et al.* 2021). As an ornamental plant with a large planting area, holly requires a large amount of pruning every year; therefore, mechanized pruning is the inevitable development trend of pruning and trimming holly. To determine the appropriate size of the holly after pruning to achieve the degree of beauty, after research and market analysis, we selected the common spherical holly (provide a rounded shape of the top part of an individual holly tree or bush, will be named spherical holly; in this paper) and straight-shaped holly (create a rectangular hedge from a row of holly trees or bushes, will be named straight-shaped holly) for research and pruning objects.

Many studies have been conducted at home and abroad on holly pruning machines and pruning technology. In terms of vision, the literature (Botterill et al. 2017; He and Schupp 2018; Kamandar et al. 2022) has made a breakthrough in the combination of vision or sensors and pruning, which to a certain extent realizes accurate pruning at precise locations and at the same time helps to improve the degree of refinement of pruning, which in turn improves the efficiency of pruning and pruning aesthetics. In terms of mechanical mechanisms, the pruners in the literature (Iwano et al. 2016; Azlan et al. 2021; Thiyagarajan 2024) use scissor-like, rotary, and a combination of moving and fixed blades, and each has its own advantages and disadvantages, with the scissor-like method being suitable for precision pruning, and the combination of rotary and moving blades is suitable for wide-area pruning. Bá lint Siktár has made a breakthrough in the combination of precise location and precise pruning to a certain extent, which helps to improve the degree of refinement, thus improving pruning efficiency and aesthetics. Siktár et al. (2024) studied a trimmer with a cam-follower mechanism, which improves the transmission efficiency to a certain extent, but lacks shape-specific trimming functions (Liu et al. 2013; Meng et al. 2013; Xu et al. 2013; Li et al. 2021; Kamandar et al. 2022) The trimmers described in the literature (Liu et al. 2013; Meng et al. 2013; Xu et al. 2013; Li et al. 2021; Kamandar et al. 2022) generally adopt a multi-degree-of-freedom design, which is a breakthrough in the trimming of hedges of different shapes, reduces the waste of time, and cost because of the frequent switching of knives, and improves the trimming precision and trimming efficiency; in the aspect of control, trimmers in the literature (Kaljaca et al. 2020; Westling et al. 2021) have a breakthrough in terms of algorithms and operation procedures, and have an innovation in terms of control and operation procedures. In terms of control, the pruners described in the literature (Kaljaca et al. 2020; Westling et al. 2021), though they indicate breakthroughs in algorithms and operating procedures, they are slow in functioning etc.; the pruners used in Qiu et al. (2024) use a PLC system for controlling the whole machine, which improves the stability and accuracy of control, and also adopt a two-stage lifting mechanism, which enhances lifting and lowering flexibility; the pruning dynamic stability in the literature (Zhan et al. 2020; Lu 2021) is improved in the experimental method. In terms of experimental methods, the pruning machine developed by Zhang et al. (2022) adopts the D-H parametric coordinate method for analysis and adopts a mechanical arm to carry out pruning work, which improves pruning flexibility. The pruning machine researched by Luo et al. (2021) has a more outstanding performance in highway hedge pruning. Luo et al. (2021) also studied trimmers with outstanding performance in highway hedge trimming, with strong adaptability to complex environments but lacking small-scale horticultural operations for farmers.

In view of the above situation, it is necessary to reduce labor costs, reduce the burden of manual pruning, and improve pruning efficiency and aesthetics. In this study, a holly pruning machine with multifunction, easy operation, and simple structure was designed.

Based on the three-dimensional design software, the model building, and key components of design were improved according to the research in this study, and finally a physical prototype was built. This machine solves the problems that some old pruning machines hold such as inefficiency to prune multiple shapes, have a low degree of automation, and have few functions. Compared with the existing machine, the machine not only can complete the different shapes of holly pruning, but also control holly pests and diseases; at the same time, the machine uses electricity as energy, clean, environmentally friendly, and is conducive to the improvement of control precision and flexibility. The holly pruning machine designed in this study is a small- and medium-sized pruning machine, convenient and flexible, compared with large pruning machines, suitable for small-scale work, both multi-scenario use, occupies a certain advantage in the market, and is convenient for gardeners to use.

EXPERIMENTAL

Overall Structure and Working Principle of Holly Pruning Machine Design

In this study, a holly pruning machine with adaptive tool adjustment was developed based on the aesthetic analysis of holly horticulture. The device uses electric servo drive system to provide power for each actuator, through the tool adaptive adjustment mechanism to realize the multi-shape pruning of holly plants, and through the PLC to realize the automatic control and remote control when pruning holly. The system integrates five functional modules: pruning, spraying, walking, ranging, and visual recognition. The modules work together through the PLC control system to meet the multi-dimensional modeling needs of holly plants in the landscape. The adaptive tool adjustment holly pruning machine adopts a reciprocating pruning tool for pruning. The main structure is as follows: power supply and control system, tool adaptive adjustment mechanism, tool lifting mechanism, pruning mechanism, vision mechanism, frame, spraying mechanism, and walking mechanism. The whole machine adopts the rack as the basic support platform, the spatial layout of the functional components is configured in the following way: the visual mechanism is arranged in an orthogonal positioning mode in the geometric center of the upper side of the box door at the front end of the rack to realize the monitoring of the operating area; the central trimming part of the trimming mechanism is fixed on the lower surface of the central load-bearing plate of the rack through the suspension device to form a vertical workspace; the lateral trimming part of the trimming mechanism is located in the box door of both sides of the rack and connected with the lateral rotating platform; the tool self-adaptive adjusting mechanism is located in the box door of both sides of the rack. With the side of the rotating platform connection, the tool adaptive adjustment mechanism using elastic coupling embedded in the trimming actuator and tool connection node to achieve dynamic adjustment of the shear attitude; spraying mechanism spray box, power supply, and control system were integrated in the frame on both sides of the box door on the bearing surface to form a symmetrical distribution of functional modules; the spraying mechanism is located in the vision agency below; the main body is located in the upper part of the box door of the frame, and the central load-bearing plate; the main organization is located in the upper box door of the frame, the central load-bearing plate. This layout ensures spatial independence of the functional modules while effectively maintaining the mass balance and structural rigidity of the entire system. The three-dimensional model of the entire machine is shown in Fig. 1.

The holly pruning machine designed in this study has the following three technical advantages: based on the problem of pruning different holly shapes, the tool adaptive adjustment mechanism can dynamically adjust the cutting angle according to the shape of the plant, realizing accurate pruning of various shapes of holly plants; based on the problem of holly shape detection and holly distance measurement, the spatial perception system of vision technology can synchronously realize the function of target detection and distance measurement; based on the problem of holly's susceptibility to diseases and pests, the spray mechanism can meet the daily spraying needs of holly plants through the modular design. daily spraying needs of holly plants, effectively controlling the occurrence of pests and diseases, and effectively preventing and controlling pests and diseases.



Fig. 1. 3D model of holly pruning machine with adaptive tool adjustment: (1) hand lever; (2) frame; (3) spraying mechanism; (4) vision mechanism; (5) pruning mechanism; (6) tool adaptive adjustment mechanism; (7) walking mechanism

The holly pruner with adaptive tool adjustment uses a design solution of visual recognition, tool adjustment, performing pruning, and additional spraying. The program has many advantages. The design is able to prune both the spherical type of holly shape and the straight type of holly bushes in a row by changing the position of the pruning tool to complete the problem of tool adaptive adjustment mechanism. The design can realize the distance measurements and holly shape recognition needs of the vision mechanism. The machine is designed to accomplish a reciprocating pruning mechanism for the pruning of the holly branches and leaves. The design includes a lifting mechanism that can meet different heights of pruning. The design of spraying mechanism can solve the problem of holly pests and diseases and realize chemical control. The design allows for remote control walking and automatic actions with an omnidirectional walking mechanism. The whole

machine uses a PLC as a control system, with a power supply to support the control system. In response to the need for manual pulling when the device is jammed or tipped over, hand levers are provided that can be readily removed and installed on the rear side of the entire machine. The primary parameters of the machine are listed in Table 1.

Table 1. Main Technical Parameters of Holly Pruning Machines with Adaptive Tool Adjustment

Technical Parameters	Numerical Value
Overall size (L×W×H) (mm×mm×mm)	1100×1450×1820
Overall machine mass (kg)	81
Tool lifting mechanism motor torque (N•m)	8.5
Maximum lifting speed of tool lifting mechanism (mm/s)	200
Tool adaptive adjustment mechanism rotating motor torque (N•m)	0.6
Tool adaptive adjustment mechanism adjusts the Angle (°)	70
Total motor power of trimming mechanism (W)	5000
Trimming mechanism cutting diameter (mm)	15
Working hours (h)	6-7

The schematic diagram of the machine design is shown in Fig. 2.

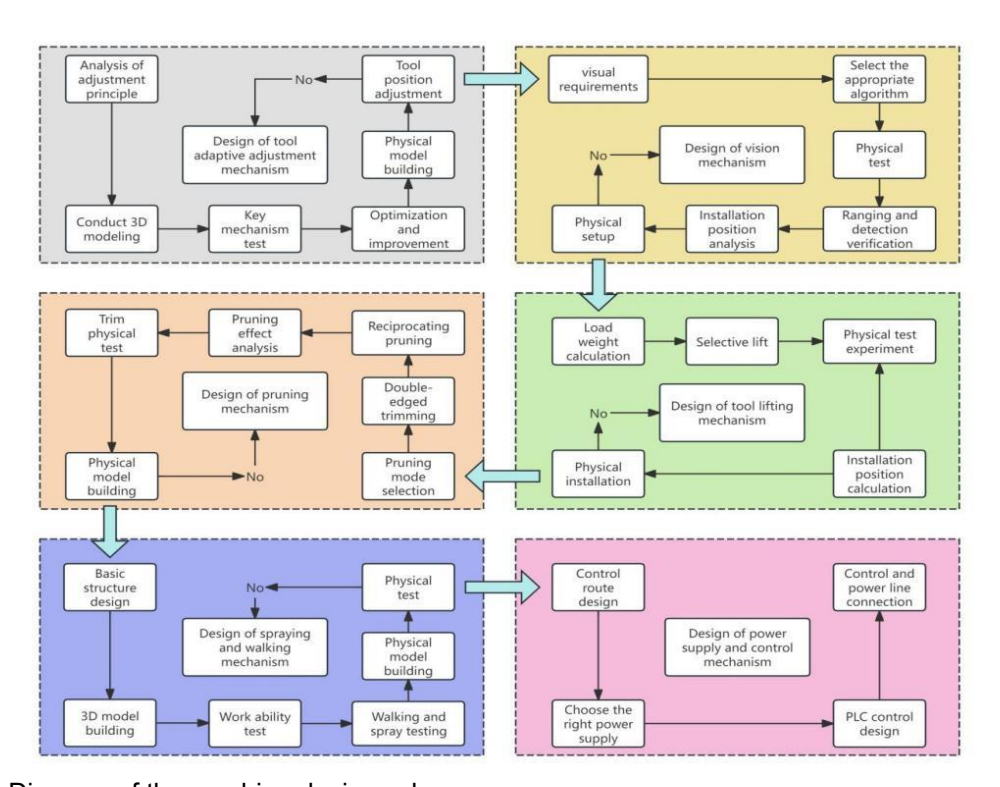


Fig. 2. Diagram of the machine design scheme

Structural Design of the Whole Machine

Investigation of holly horticultural pruning parameters and dimensioning of pruning mechanisms

For spherical holly and straight holly, multi-region, multiple ground research, measurements to obtain a number of groups of shape parameters of the normal growth state of holly, and the use of box plots for drawing, a number of groups of parameter measurements are shown in Fig. 3. The physical and shape depiction of spherical and straight holly is shown in Fig. 4.

Some discrete parameter measurements were removed, and more concentrated parameter measurements were selected to delineate the size parameter ranges and finalize the general holly horticultural pruning size ranges, as shown in Table 2.

Table 2. General Holly Horticultural Pruning Size Range

Shape	Diameter or Width (mm)	Height (mm)	Angle (°)
Bulbous Holly	1100 to 1200	1300 to 1400	1
Straight Holly	900 to 1100	800 to 1200	65-85

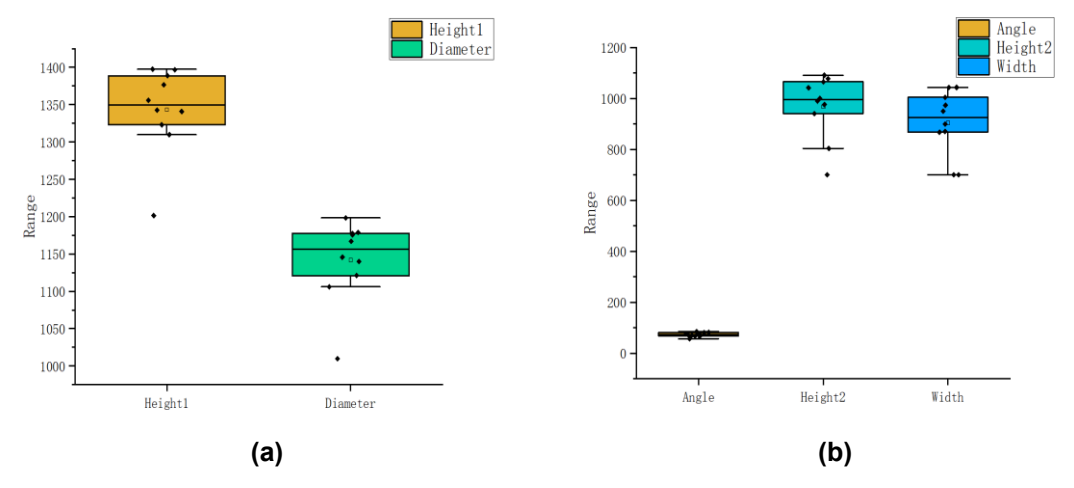


Fig. 3. Measurement results of shape parameters of holly:(a) Measurement results of shape parameters of spherical holly; (b) Measurement results of shape parameters of straight holly

Based on the statistical analysis of the box and line graph, the average value of the parameters in the size range of holly horticultural pruning was obtained; the average value of the diameter of the spherical holly was 1160 mm, the average height was 1360 mm; the average width of the straight holly was 960 mm, and the average height was 1025 mm. By combining the diameters and widths of the spherical holly and the straight holly, the average value was again calculated, resulting in an average width or diameter of 1060 mm, The average height value after the combination of the average value of 1190 mm, and the test of variance, resulting in the calculation of the variance value which is within a reasonable range, and the data are distributed in the box and line graph in more than 80%, in line with the degree of dispersion of the requirements of holly pruning. Considering that the plant will grow after pruning, the machine will be pruning the maximum width (diameter) is set to 1000 mm, the value and the average value of the difference, the test, in line with the requirements of pruning, combined with the plants in the growth process of the apical dominance and the ground slope of the different in order to expand the pruning

range, the maximum pruning height is set to 1150 mm. Combined with the apical dominance of plants in the growth process and the different slopes of the ground, the maximum pruning height of the machine was set to 1650 mm to expand the scope of pruning.

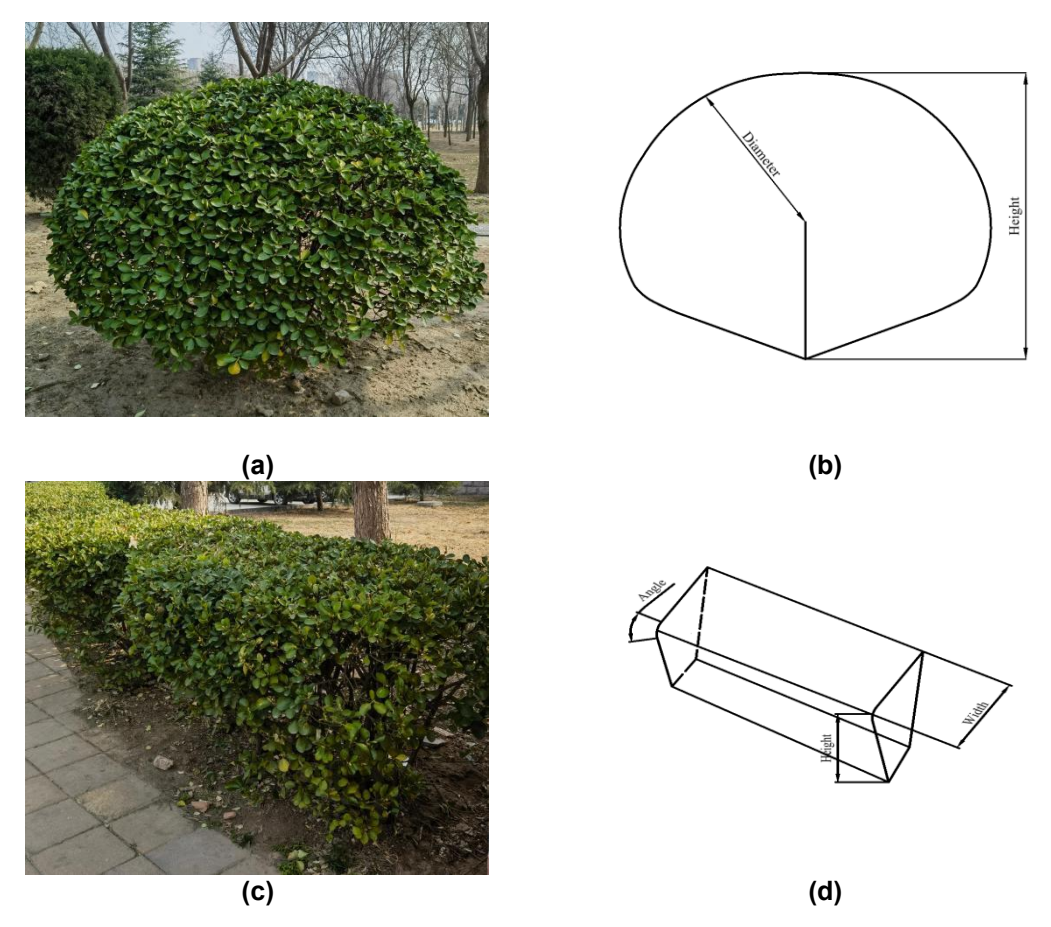


Fig. 4. Holly physical and shape depiction diagrams: (a) spherical holly physical diagram; (b) spherical holly shape depiction diagram; (c) straight holly physical diagram; (d) straight holly shape depiction diagram

The power of the pruning mechanism is mainly provided by a 24V DC motor, which can realize the pruning of holly branches and leaves. The trimming mechanism can realize brushless three-stage speed regulation, a trimming mechanism start-stop, and three-stage speed regulation through PLC control. According to the pruning needs and the overall size of the machine, because the length of the drive housing is 200 mm, the pruning mechanism of the upper pruning tool length is set to 665 mm, the lower pruning tool length is set to 481 mm, the side of the tool length is set to 600 mm, and the length of the proportional arrangement of the pruning mechanism can not only increase the pruning tool pruning effective pruning area, but also ensure that the pruning mechanism of the position of the tool in the tool adaptive adjustment mechanism is adjusted under normal pruning. Such a setup, on the one hand, is conducive to improving the pruning efficiency; on the other hand, it can improve the pruning operator's unnecessary second pruning (the second pruning refers to the first pruning after the existence of missing pruning or machine cannot be pruned to the place, need to manually compensate for pruning).

Mechanical Analysis of Pruning Blade Interaction with Holly Branches

In order to reveal the mechanism of interactions between the pruning tool blade and holly branches, according to the principle of decomposition of spatial force system, firstly, the spatial force F is decomposed into the horizontal force F projected onto the x-y plane and the force F along the z-axis direction (*i.e.*, the pressure of holly branches and leaves on the movable edge or fixed edge), and then, the horizontal force F is decomposed into the shear force F and the sliding force F along the x-axis and the y-axis respectively as shown in Fig. 5.

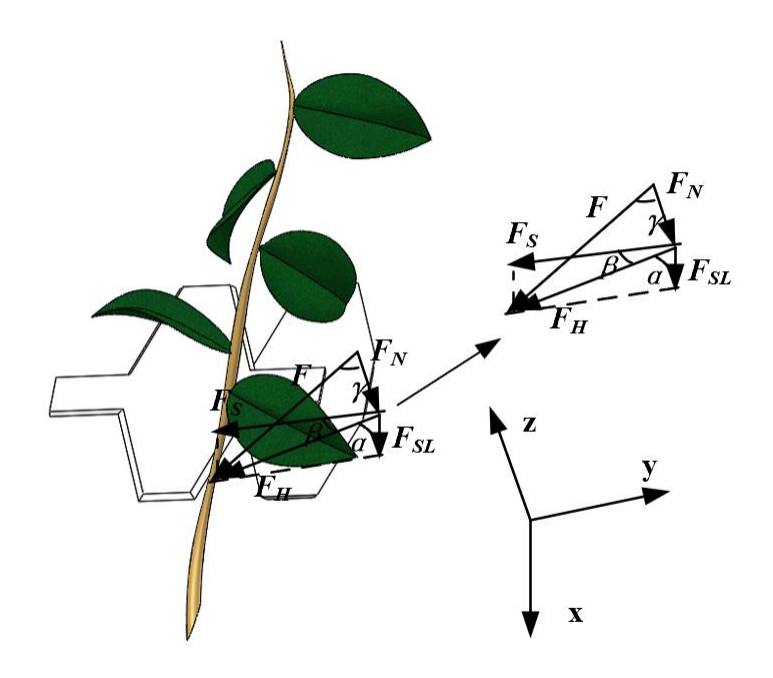


Fig. 5. Mechanical analysis diagram of pruning tool blade interaction with holly branches.

According to the principle of synergistic action of the shear force and the double-edged synergistic principle to analyze, the equation can be made,

$$F_{S} = F_{H} \cdot \cos \beta = F \cdot \sin \gamma \cdot \cos \beta \tag{1}$$

$$F_{SL} = F_H \cdot \cos \alpha = F \cdot \sin \gamma \cdot \cos \alpha \frac{\pi}{2}$$
 (2)

$$F_{SL} = F_f = \mu \cdot F_N \tag{3}$$

where F_S is the shear force (N), F_H is the horizontal force (N), F is the spatial force (N), α is the angle between F_H and F_S (°), β is the angle between F_H and F_S (°), γ is the angle between F_N and F (°), F_{SL} is the sliding force (N), F_N is the pressure of holly branches and leaves on the movable or fixed edge (N), F_f is the friction of the blade against holly branches and leaves (N), μ is the dynamic friction factor of the blade.

In order to solve the shear force and friction force generated by holly branches and leaves, the approximate value of the maximum spatial force F on the knife blade was used to calculate 850 N (where the γ angle was approximated to be 75 °, the β angle was approximated to be 25 °, the α angle was approximated to be 65 °, and the kinetic friction factor of the knife blade was 0.56), which was brought into the above equation to obtain the shear force of 744 N and the friction force of 123 N. It is verified that the friction force is smaller than the slipping force of 200 N, which is very easy to slip when pruning. The

friction force of 200 N can prevent holly branches and leaves from slipping instantly during pruning and reduce the accuracy of shape pruning. By these means it can complete the pruning of holly branches.

Design and Analysis of Adaptive Tool Adjustment

To solve the problem of pruning holly shapes at different heights, combining tool adjustment and pruning mechanism lifting and lowering, the tool adaptive adjustment mechanism and lifting mechanism are designed to expand the pruning range, improve the pruning efficiency, and enhance the aesthetics of holly pruning horticulture. The tool lifting mechanism consists of a screw module, support rod, and central bearing plate. The tool adaptive adjustment mechanism consists of a vertical guide rail group, actuator motor, rotating platform, horizontal slider group, vertical slider group, bearing group, and tool slidable connecting plate. The three-dimensional structure of the adaptive adjustment mechanism of the tool and the lifting mechanism are shown in Fig. 6.

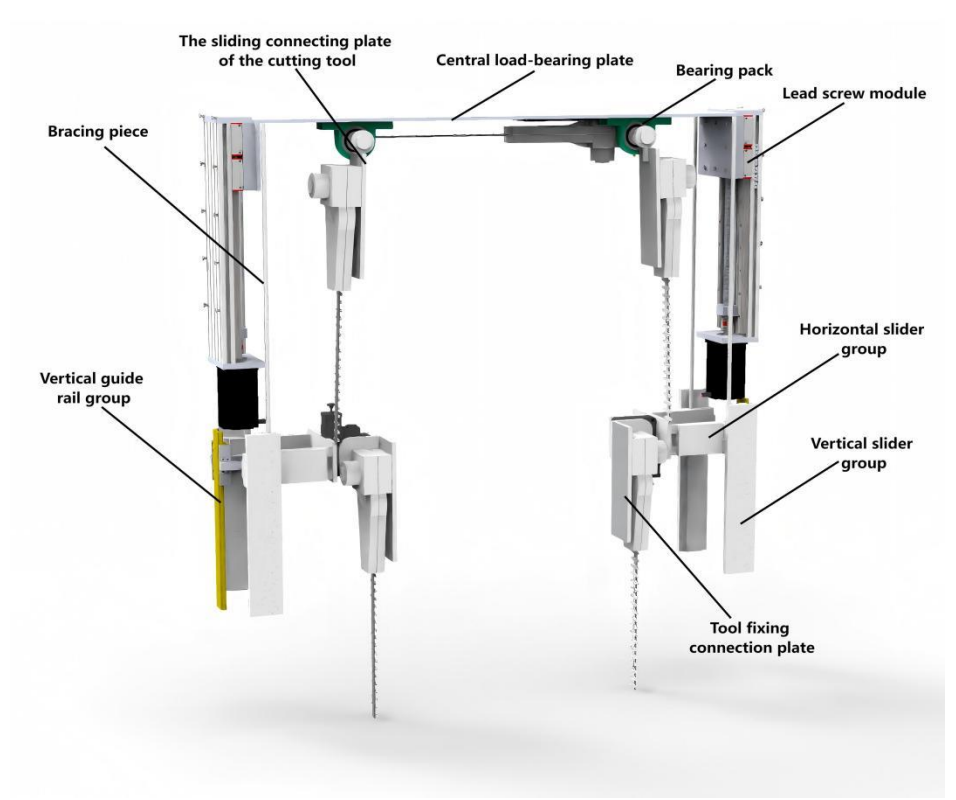


Fig. 6. Three-dimensional structural diagram of the tool adaptive adjustment mechanism and the lifting mechanism

Tool Adaptive Adjustment Mechanism Analysis

The purpose of the tool adaptive adjustment is to adaptively adjust the position of the tool according to the shape recognized by the binocular vision mechanism when pruning different shapes of hollies, so as to reduce the time and physical strength spent by the operator when switching between different shapes of hollies when they need to prune or make different movements, and ultimately to realize the enhancement of pruning efficiency.

According to the characteristics of the tool adaptive adjustment mechanism, because of its symmetrical structure, so the analysis of one side of the structure, the use of

institutional motion sketch of the tool adaptive adjustment mechanism for motion characterization, as shown in Fig. 7, components 1, 2, and 3 together constitute a vertical slider group and vertical guide group; components 4 and 5 for the actuator motor; components 6, 7, and 11 together constitute a horizontal slider group; components 8, 9, respectively, for the trimming. The members 8 and 9 are the lower and upper cutters of the trimming mechanism respectively; the member 10 is the sliding connecting plate of the cutter.

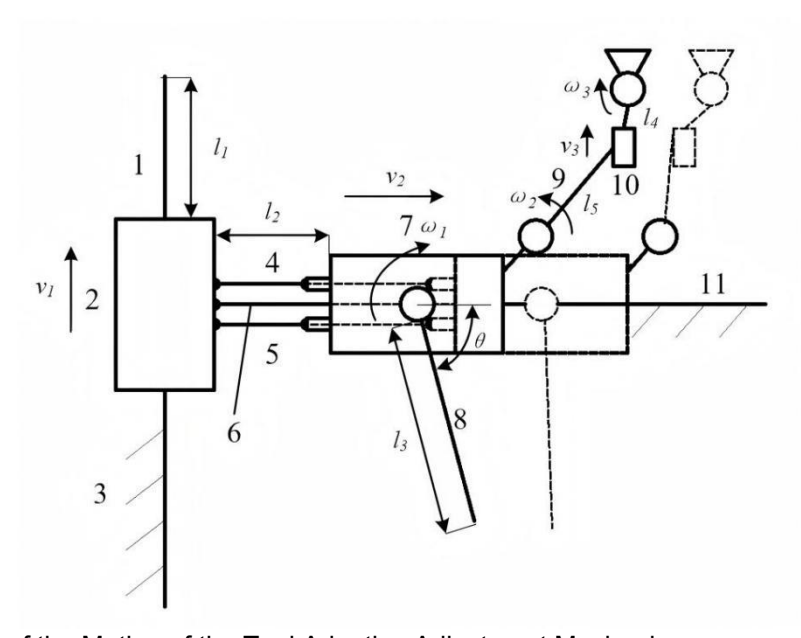


Fig. 7. Sketch of the Motion of the Tool Adaptive Adjustment Mechanism.

According to the principle of kinematics of the mechanism, combined with the motion sketch of the mechanism, the motion relationship is expressed as follows:

The line velocity of member 8 is

$$v_{8} = \omega_{1} \cdot l_{3} \tag{4}$$

where ω_l is the angular velocity (mm/s) of the rotating platform and l_3 is the lower tool length (mm) of the trimming mechanism.

It can be observed from this equation that the variation in the lower tool angle θ is mainly related to the rotating head.

The linear velocity of member 9 is

$$v_{q} = \omega_{2} \cdot l_{5} \tag{5}$$

where ω_2 is the angular velocity due to the horizontal actuator drive and l_5 is the length of the tool on the trimming mechanism.

The velocity of member 9 on member 10 is (let the angle between member 9 and the horizontal be α).

$$v_{3} = v_{0} \cdot \cos \alpha \tag{6}$$

The linear velocity at the connector above member 10 is

$$v_{i0} = \omega_3 \cdot l_4 \tag{7}$$

where ω_2 is the angular velocity due to the horizontal actuator drive and l_5 is the length of the tool on the trimming mechanism and (let the angle between the connection above member 10 and the horizontal direction be γ).

$$v_{10} = v_3 \cdot \cos \gamma \tag{8}$$

The relationship between the actuator motor speed v_2 and the angular velocity ω_2 is (let the length at the center of rotation of angular velocity ω_2 where it joins the center of the member, be s)

$$v_2 = \omega_2 \cdot s \tag{9}$$

According to Eqs. 4-9, it can be obtained that

$$v_{10} = \frac{v_2 \cdot l_5}{s} \cdot \cos \alpha \cdot \cos \gamma \tag{10}$$

According to Eq. 10, it can be concluded that the linear velocity at the connection member above the slidable connection plate (member 10) of the tool is the result of the actuator motor drive, and the magnitude and direction of its value are mainly related to the actuator motor speed, length of the connection between the center of rotation at the angular velocity ω_2 and the center of the member, length of the tool on the trimming mechanism, angle of member 9 in the horizontal direction, and angle of the connection member above member 10 in the horizontal direction. Combined with the above kinematic analysis, the feasibility and rationality of the push rod motor driving the relevant parts of the tool adjustment mechanism were verified.

Simulation Analysis of Tool Adaptive Tuning

The three-dimensional model of the tool adaptive adjustment related institutions was imported into Adams 2018 software on different shapes of holly pruning and adjustment process for kinetic simulation drive and connecting vice to create the completion of the diagram shown in Fig. 8.

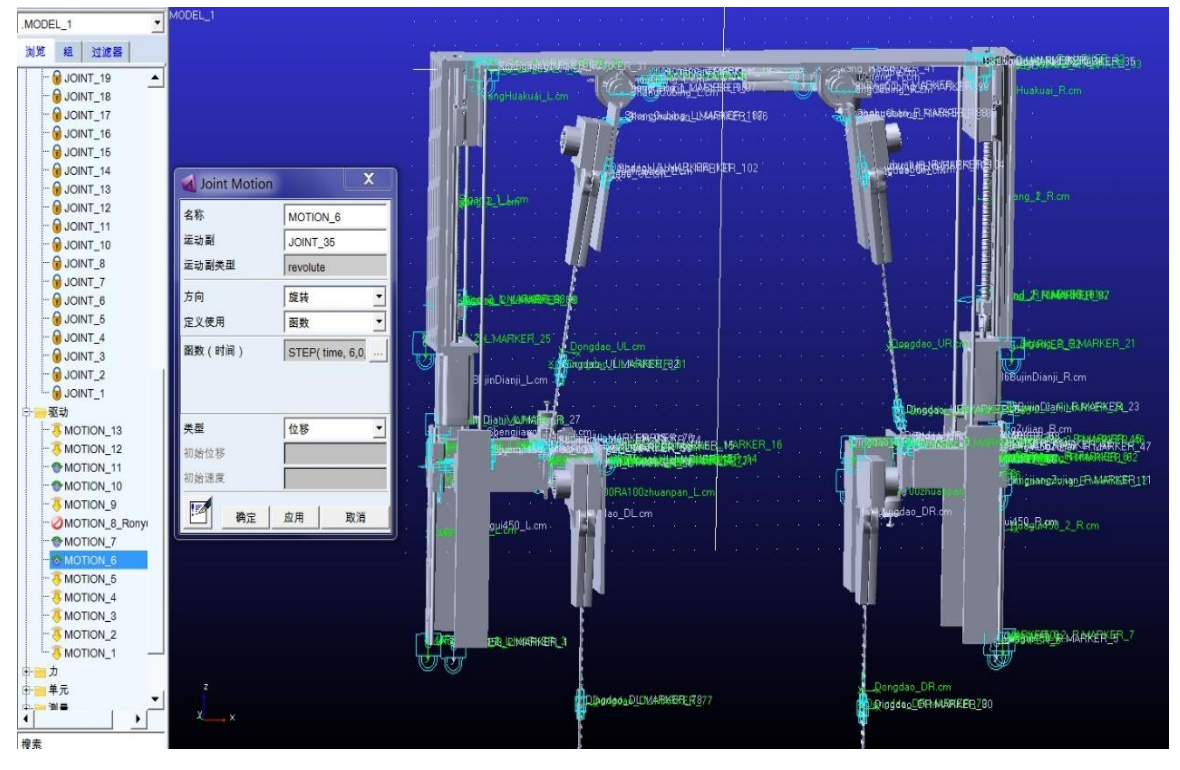


Fig. 8. Diagram of the relationship between the driving and connecting subsystems of the mechanism related to the adaptive adjustment of the tool

After establishing the connection relationship and drive, setting the duration movement time as 12 s and the number of steps to 500, the kinematic interaction simulation dialog box is shown in Fig. 9. According to the different adjustment and trimming actions, the above two parameters are adjusted, and the kinematic simulation is carried out.

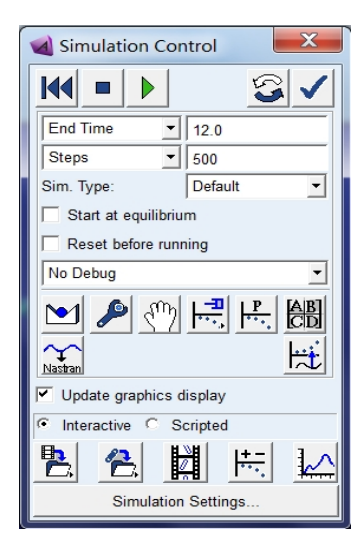
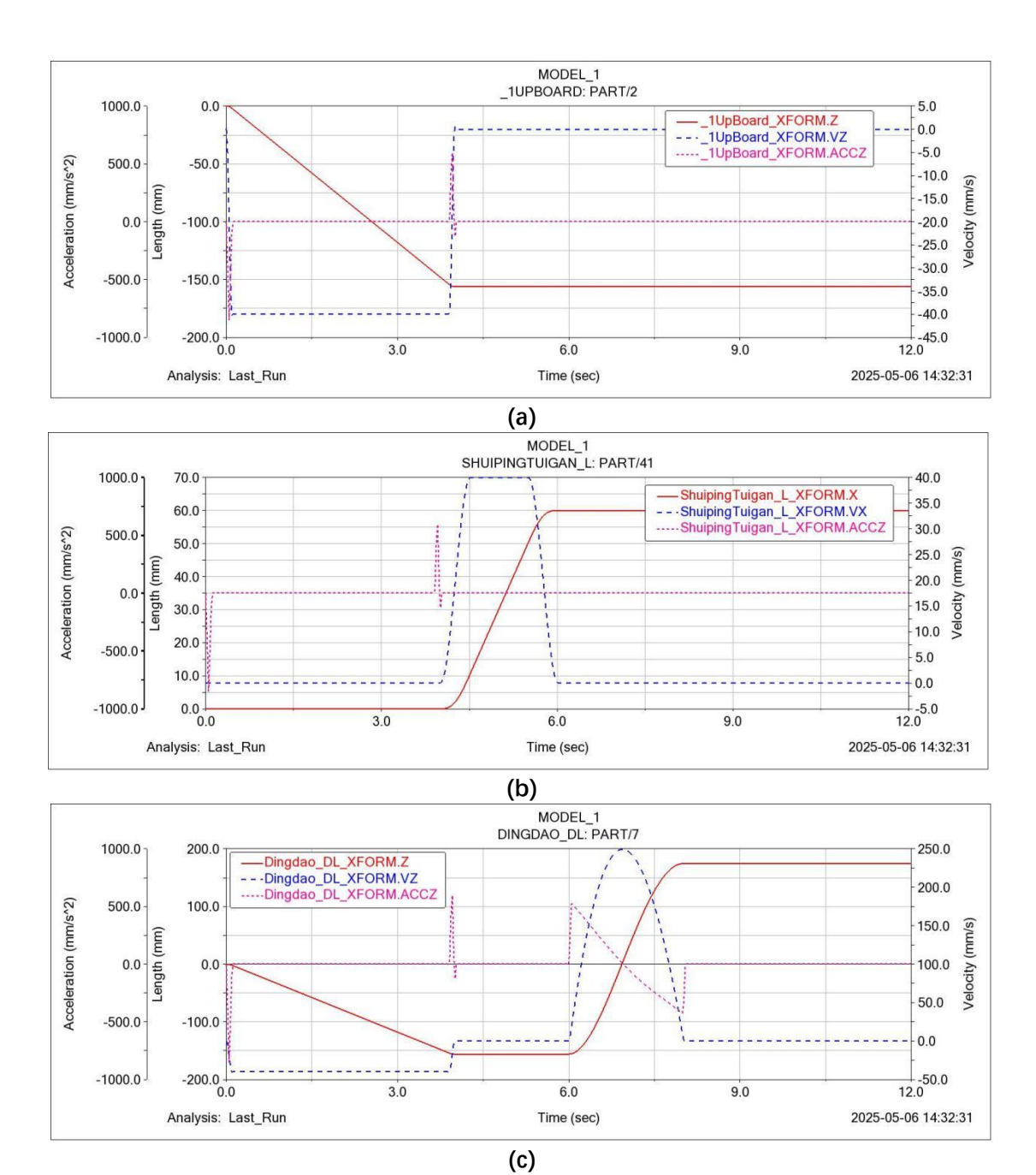


Fig. 9. Kinematics Interactive Simulation dialog box

After completing the kinematic simulation, the post-processing of the tool adaptive adjustment tool was completed in the Adams 2018 software. First, all the driven functions were adjusted, the time allocated to ensure the integrity of the simulated action was allocated, the simulation was performed, and the post-processing operation was carried out to obtain the displacement, velocity, and acceleration graphs of the target part (trimming of the spherical holly, set the trimming height of 1350 mm), as shown in Fig. 10.

The displacement (Z), velocity (VZ), and acceleration (ACCZ) of the tool lifting mechanism are shown in Fig. 10a. The displacement of the lifting mechanism increased linearly with the increase of time over the distance of 160 mm. The velocity of the lifting mechanism is in the interval of 40 mm/s at the beginning, and it reaches the specified position and the velocity decreases to 0 after 4 s. The acceleration of the lifting mechanism is in the range of 0, and some fluctuations occur near 0 s and 4 s The acceleration of the lifting mechanism is at 0, with some fluctuations around 0s and 4s, which are mainly variations caused by the start and stop of the motor. The displacement (X), velocity (VX) and acceleration (ACCZ) of the actuator motor are shown in Fig. 10 b. In the initial time range 0 to 4 s, the horizontal actuator stays motionless, and its displacement, velocity, and acceleration are all 0. In the 4 to 6 s time range, the displacement of the horizontal actuator shows a linear increasing trend with the increase of time. According to the velocity curve, the horizontal pusher experienced accelerated motion, 40 mm/s uniform velocity motion, decelerated motion, and finally reached the target position to stop. The displacement (Z), velocity (VZ) and acceleration (ACCZ) of the tool under the trimming mechanism are shown in Fig. 10 c, and the displacement and velocity-acceleration curves of the tool are consistent with the curve changes of the lifting and lowering assembly in the 0 to 4 s range. In the 4 to 6 s range, the lifting assembly reaches the specified height, and each value is 0. In the 6 to 8 s range, the adjustment of the lower tool angle is started because the direction of the tool angle adjustment is opposite to the direction of the lifting assembly, and the adjustment of the lower tool angle increases the displacement curve in the opposite

direction. The displacement (Z), velocity (VZ), and acceleration (ACCZ) of the moving edge of the lower tool of the trimming mechanism are shown in Fig. 10 d, and the displacement, velocity and acceleration curves of the moving edge during 0 to 4s are consistent with the curve changes of the lifting mechanism. In the 6 to 8 s range, the displacement, velocity and acceleration curves are consistent with the curve change of the lower tool. In the 8 to 12 s range, the tool starts to reciprocate, and the displacement, velocity and acceleration curves of the movable edge all show the law of periodic change to realize the action of cutting holly branches and leaves.



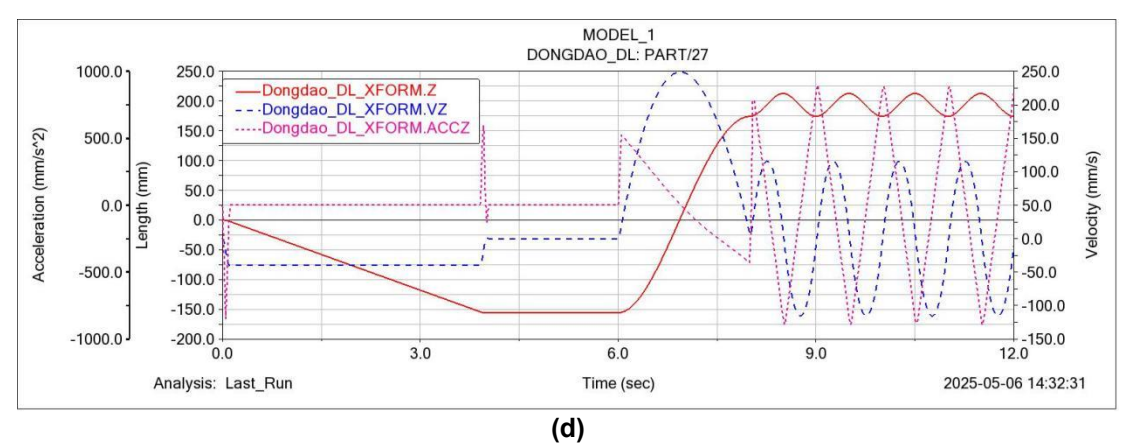


Fig. 10. Displacement, velocity, and acceleration graphs of target components: (a) Displacement, velocity and acceleration graphs of the tool lifting mechanism; (b) Displacement, velocity and acceleration graphs of the actuator motor; (c) Displacement, velocity and acceleration graphs of the tool under the trimming mechanism; and (d) Displacement, velocity and acceleration graphs of the tool's moving edge under the trimming mechanism

Visual Organization Design and Analysis

The vision mechanism was located at the front of the holly pruning machine frame on the upper side of the upper box door at the center. The hardware mainly adopts a binocular vision setup and CoreVision camera module. The mechanism mainly adopts high-precision (millimeter-level) binocular synchronization with the same frame; in terms of the algorithm, it mainly adopts the SGBM algorithm, which combines the holly leaf texture characteristics to design the adaptive matching window. The experimental results showed that the average relative error of the system was controlled within 1.2% in the effective range of 0.5 to 3 m, and the leaf area measurement accuracy reached 97.8%, which is significantly better than that of the monocular vision measurement method (P<0.01).

When performing ranging, the main process is the system calibration module, followed by binocular image acquisition and preprocessing, followed by the improved SGBM stereo matching algorithm process. Finally, depth calculation and subsequent processing, the vision mechanism ranging flowchart is shown in Fig. 11.

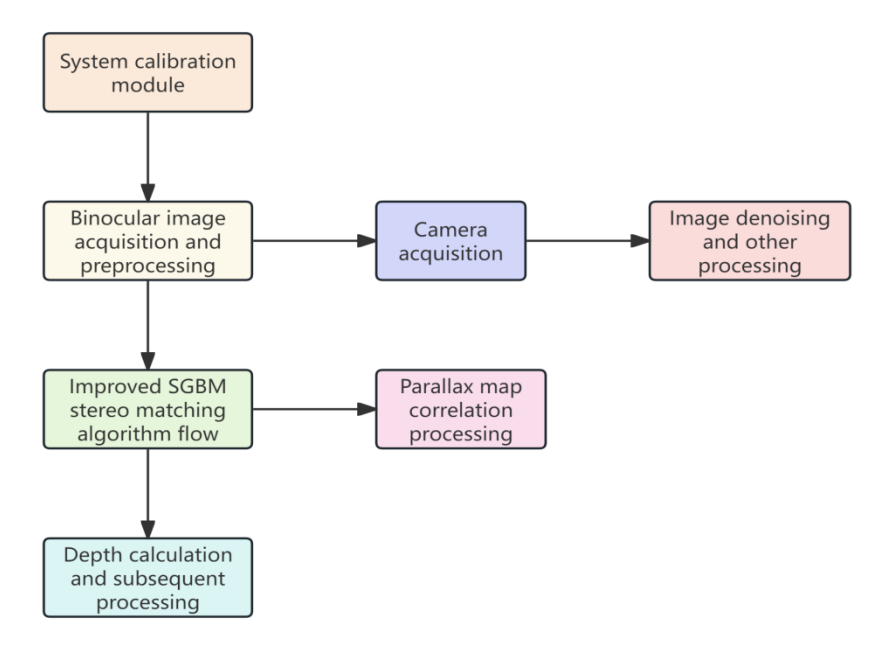


Fig. 11. Flowchart of the vision mechanism ranging process

For example, according to the SCBM algorithm, the camera first performs image acquisition. The left eye image is shown in Fig. 12a, and the right eye image is shown in Fig. 12b. The pseudo-color map generated using the algorithm is shown in Fig. 12c, and the generated parallax map is shown in Fig. 12d.

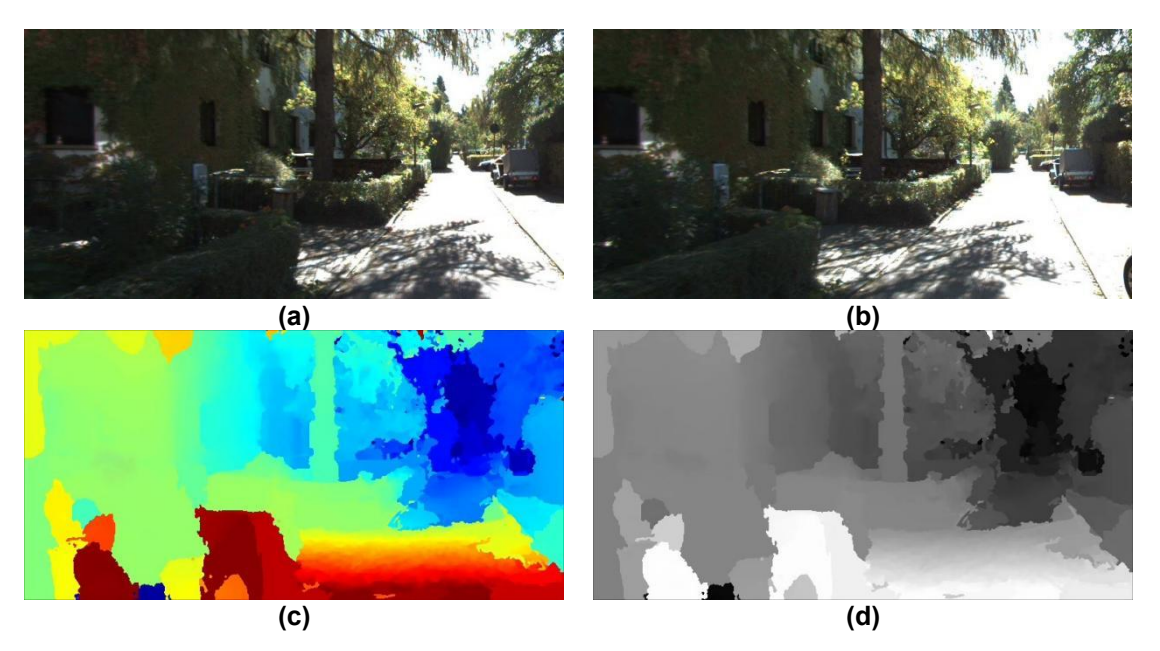


Fig. 12. SGBM algorithm ranging maps: (a) left-eye image; (b) right-eye image; (c) pseudo-color map; (d) parallax map.

Based on the improved YOLOv5 algorithm, a dedicated image dataset for a straight and spherical holly were constructed and combined it with targeted data enhancement strategies to effectively improve the model's ability to recognize target features. For the multi-target interference problem in complex agricultural and forestry scenes, dynamic confidence threshold, and category filtering mechanisms are adopted to actively screen out non-target objects in the post-detection processing stage, so that the model focuses on key detection tasks. In the training process, the parameters recommended by YOLOv5 were selected, and the resulting changes in the indicators during the training process are shown in Fig. 13. It can be concluded that the accuracy rate was maintained between 60% and 80%, the difference between the detection frames was no more than 0.02, and the loss value was ultimately no more than 0.01, which met the detection requirements.

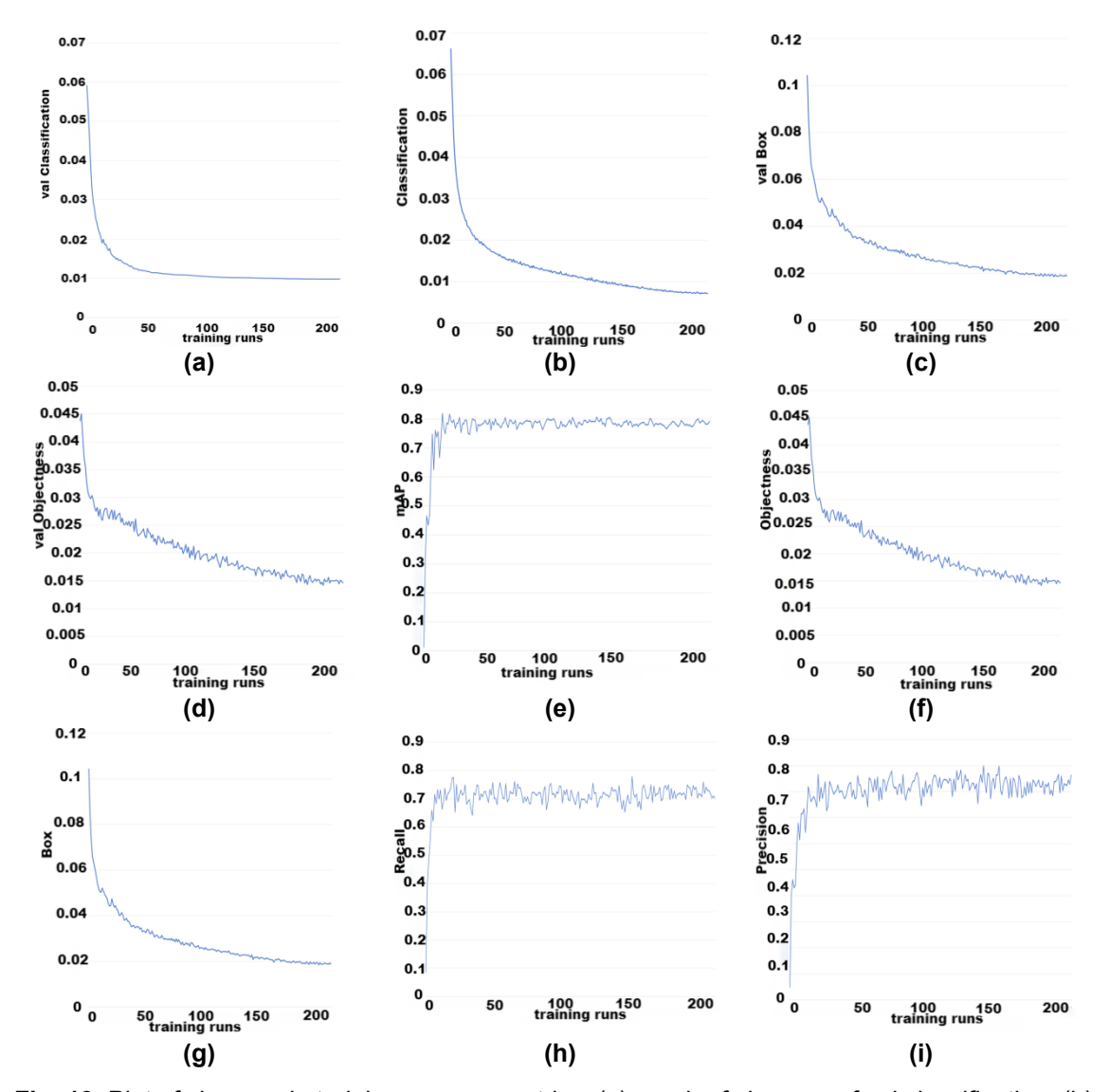


Fig. 13. Plot of changes in training process metrics: (a) graph of changes of val classification; (b) graph of changes of classification; (c) graph of changes of val box; (d) graph of changes of val objectness; (e) graph of changes in mAP; (f) graph of changes of objectness; (g) graph of changes of box; (h) plot of change in recall; (i) accuracy change graph

Experiments showed that the method maintained the original real-time advantages of YOLOv5, while the average detection accuracy was improved by 12.6% compared with the baseline model. By optimizing the non-great suppression parameter and the weight allocation of the loss function, it significantly reduces the false detection rate of the similar

morphology of the plant and provides reliable technical support for automated morphology analysis and accurate management of holly plants, and the detection of the spherical holly at a distance of 185.3 cm was achieved. Target detection was performed, and the sample target detection diagram of the spherical holly is shown in Fig. 14.



Fig. 14. Example images of spherical holly target detection: (a) original image of spherical holly; (b) image after adding the algorithm

Combined with the recognition of the visual mechanism, it can effectively improve the adjustment accuracy of the tool adaptive adjustment mechanism, thus effectively improving the trimming accuracy and improving the trimming aesthetics.

Spraying Mechanism Design and Analysis

Setting up the spraying mechanism can be used for the prevention and control of holly pests and diseases, and at the same time, it can increase the auxiliary function of the holly pruning machine, and better utilize the spare space of the holly pruning machine. In the process of pruning holly, the machine not only can complete the pruning of holly, but it can also solve the discovery of holly disease and pest spraying pesticide work, at the same time, in order to prevent the visual mechanism from being polluted by the liquid, the nozzle can be realized to lift and lower, the spraying mechanism mainly consists of the main spraying body and the storage tank, the main spraying body consists of the spraying motor, spraying rod, the nozzle lifting module, and the nozzle composition.

After the start of the spraying mechanism, the nozzle first retracts backward, after which the nozzle-lifting module starts to work, and the nozzle descends to the bottom of the box door on the frame, after which the nozzle starts to carry out the work.

Combined with the relevant knowledge of fluid mechanics for spraying flow analysis, Bernoulli's equation, and the continuity equation, the nozzle flow equation can be introduced as,

$$Q = C_d A \sqrt{\frac{\Delta P}{\rho}} \tag{11}$$

where Q is the nozzle flow rate (m³/s), C_d is the flow coefficient of the nozzle, A is the cross-sectional area (m²) of the nozzle, ΔP is the pressure difference before and after the nozzle (Pa), and ρ is the fluid density (kg/m³).

Because the radius of the circular nozzle is 0.01 m, the flow coefficient is 0.8, the pressure difference between the nozzle inlet and outlet is measured to be 0.24 Pa, the density of the liquid is approximated to be 1, 000 kg/m^3 , and the flow rate approximation can be derived to be 1. $37 \times 10^{-6} \text{ m}^3/\text{s}$ according to the Eq. 11. In order to make sure that the liquid can be sprayed for 4 h continuously, 2 storage boxes with a size of 200 mm×240 mm×410 mm were selected to be used for storing the drug. Two 200 mm×240 mm×410 mm storage tanks were used to store the medicines.

To study the appropriate spraying range, a schematic diagram of the spraying range was drawn, as shown in Fig. 15, and the relevant analysis was carried out.

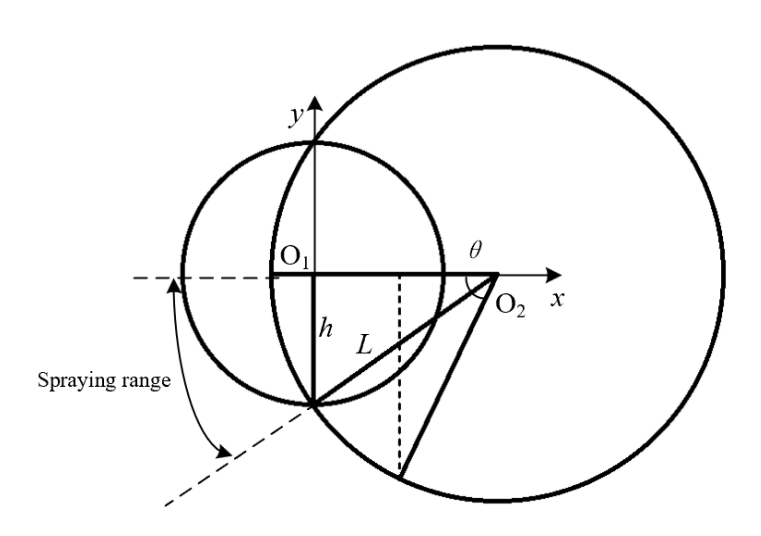


Fig. 15. Schematic of spray coverage

The spray angle can be calculated from the above figure, according to the radii of the two circles h and L, respectively. The spray angle is set for half of θ by the collinear theorem to obtain,

$$O_1O_2^2 = L^2 - h^2$$
 (12)

$$\tan\frac{\theta}{2} = \frac{h}{L^2 - h^2} \tag{13}$$

where θ is the spray angle.

According to Eqs. 12 and 13 can be calculated that the most suitable angle θ of the nozzle is 39.5°.

According to the above equation calculation and schematic analysis, the calculated data were used to perform hydrodynamic simulations in the ANSYS 2021 software Fluent module, which resulted in the pressure cloud diagrams (a, b) and velocity cloud diagrams (c, d) of the spherical holly (simulated height of 1350 mm, diameter of 1100 mm) and straight holly (simulated height of 1120 mm, width of 950 mm). Particle distribution cloud diagrams (e, f) are shown in Fig. 16.

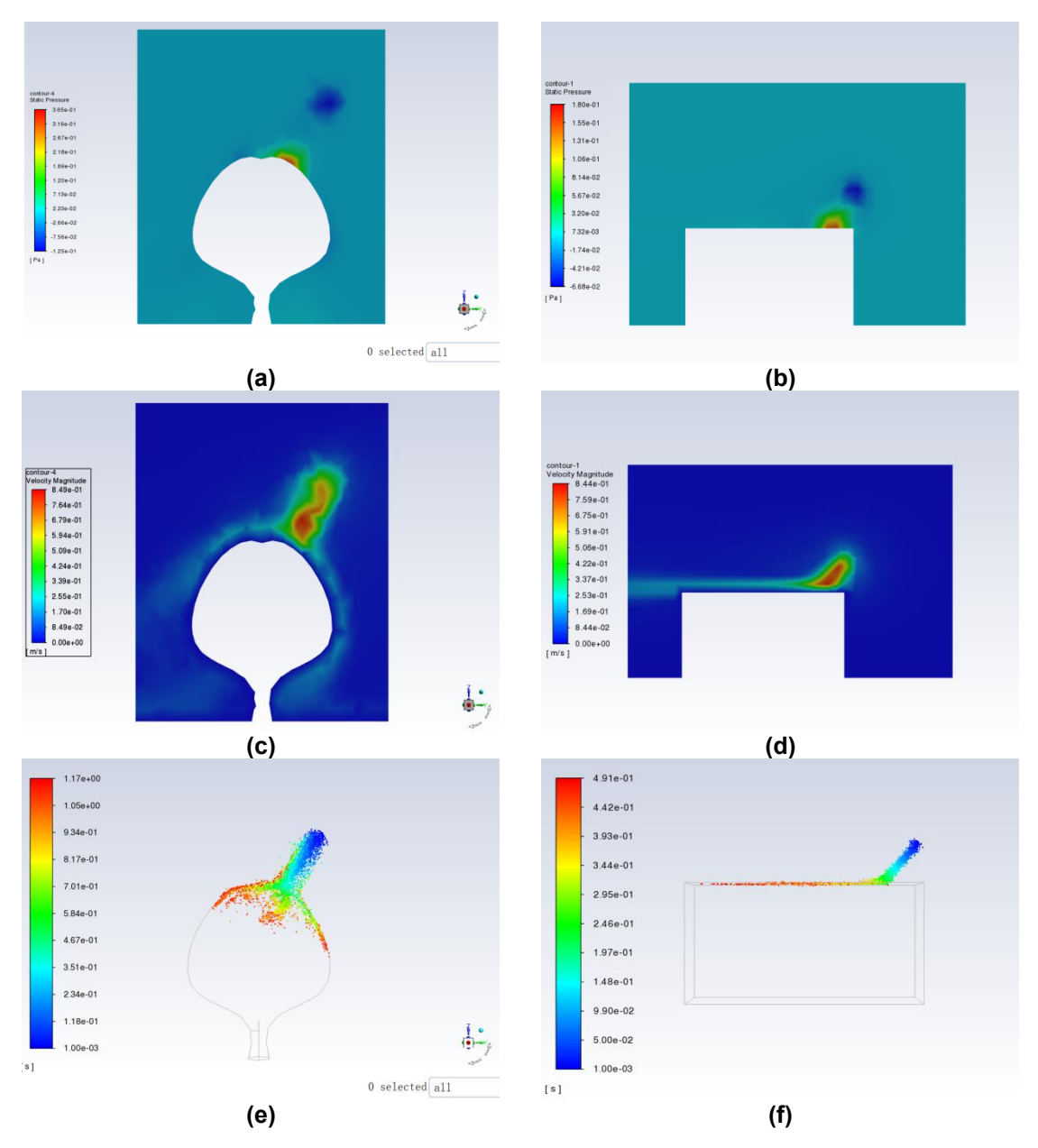


Fig. 16. Hydrodynamic simulation of spraying mechanism

According to Fig. 16, it can be seen that the pressure cloud diagram (a, b, the left side is the pressure distribution value) indicates that the pressure of the nozzle jet hitting the holly branches and leaves is high, and owing to the velocity reduction at the location, the velocity is high and the pressure is low at the source of the nozzle. The velocity cloud diagram (c, d, where the left side is the velocity distribution value) indicates that there is a significant change in the velocity after jetting, and the formation of a velocity ring around the holly, with a clear atomization effect. The particle distribution cloud diagram (e, f, where the left side is the retention time of the particles) shows that the particles are dispersed on the surface of holly branches and leaves, the distribution is uniform, and the atomization effect is good. After simulation verification, the spraying mechanism met the working requirements.

At the same time, field experiments were carried out to verify that the liquid solution could reach the leaves of the holly with ideal effects and meet the design requirements of the spraying mechanism.

Control System Design

The holly pruning machine adopted the PLC as the control system of the entire machine, which was placed in the electric control box with the power supply of the whole machine. The machine used hardware control related to three Mitsubishi PLC FX3U-16MT programmable controllers, two sets of 86 stepper motor drivers (Model: DM860H), four sets of 42 stepper motor drivers (Model: DM542), four sets of 60 servomotor drivers (Model: ES100Q-3A), actuator motor driver module and limit switches, trimming mechanism motor driver module, and electric spray gun driver module, and an electric spray gun drive module. The controller was connected to an 86-stepper motor driver for the control of the lifting mechanism, 42-stepper motors for the control of the rotating platform, and a driver module for the control of the push rod motor and the start/stop and three-stage speed change of the trimming mechanism, which controls the spraying sequence of the spraying mechanism through a solid-state relay.

To ensure the safety of the entire machine, power circuit and control circuit isolation design, emergency stop dual circuit design, and fast fuse with an electronic circuit breaker for overcurrent protection are required.

The machine vision mechanism used the YOLO v5 target detection algorithm to complete the morphological identification of holly plants. The detection data packet contained morphological parameters through the PROFINET bus to the main control unit of the programmable logic controller (PLC). The PLC was based on the structured text (ST) programming language for logical parsing, when the morphological classifiers determine that the holly is a ball-shaped, triggering the adaptive adjustment of the tool. When the morphological classifier determines that it is spherical holly, the tool adaptive adjustment of the tool is triggered by the coordinated action of the mechanism and the lifting mechanism, and the tool group is driven to complete the configuration of the spherical holly parameters. If it is recognized as a straight holly by feature matching, the tool position adjustment is realized by the PID position control algorithm. After completing the reconfiguration of the tool form, the vision mechanism starts ranging to implement the image acquisition of the target plant, and the distance parameters are uploaded to the PLC data buffer in real time through the SGBM algorithm. The central processor constructs the start-stop timing logic of the pruning mechanism and simultaneously sends motion control commands to the walking mechanism through the EtherCAT communication protocol. Among them, the traveling mechanism dynamically switches the differential steering mode or linear trajectory mode according to the target azimuth deviation value, and the trimming mechanism activates the trimming within the preset safety threshold, thus forming a complete control loop including visual perception, decision control execution, and control loop. A schematic is shown in Fig. 17.

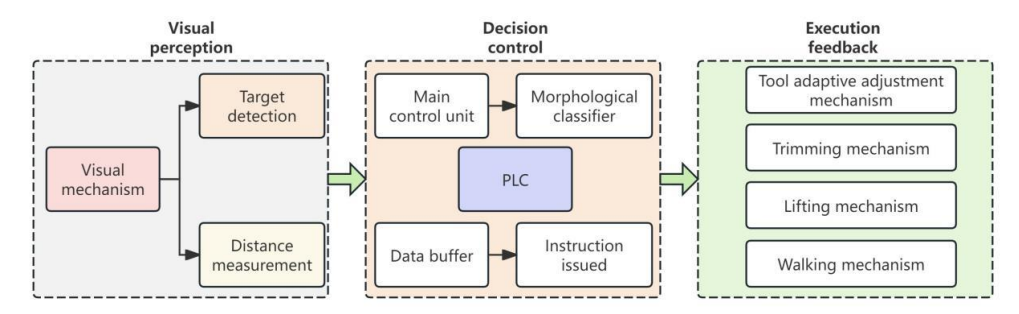


Fig. 17. Schematic diagram of the control loop.

The whole machine realizes the sequence control of each mechanism through the PLC. The first specific process involves manually starting the power supply. The traveling mechanism is controlled remotely to reach the specified position. Secondly, the vision mechanism starts to measure the distance and detect the target, and feeds the information to the tool adaptive adjustment mechanism, elevation mechanism and walking mechanism through PLC. Finally, the tool adaptive adjustment mechanism and the lifting mechanism cooperate to adjust the walking mechanism according to the shape of the holly to rotate or straight walking, with the pruning mechanism to complete the normal pruning of holly. If spraying operation is needed, after the manual start, the PLC controller controls the relay and nozzle lifting module to complete the normal work of the spraying mechanism. If encountered holly pruning machine is not able to enter the road, then the pruning is accomplished by a manual start. This uses the side box door of the side pruning mechanism, combined with visual recognition and rotary platform rotation, with the walking mechanism to carry out the holly pruning. The timing diagram of the machine work is shown in Fig. 18.

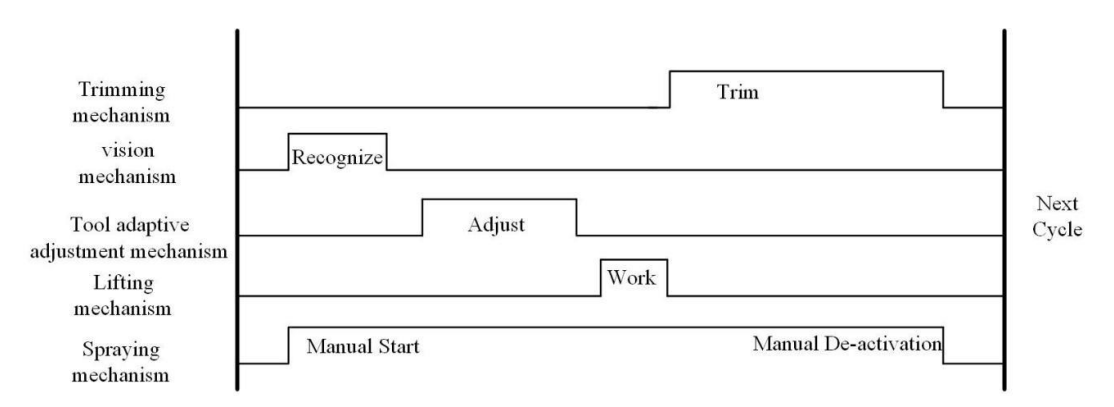


Fig. 18. Timing diagram of machine operation

RESULTS AND DISCUSSION

Experimental Materials, Conditions, and Equipment for Holly Pruning Machines

To complete the final test experiments of the machine, and to test whether the spraying mechanism, tool adaptive adjustment mechanism, and pruning mechanism can work properly, the pruning mechanism, spraying mechanism, lifting and lowering

mechanism, and tool adaptive adjustment mechanism were tested in the green belt in front of the Engineering Training Center on the campus of Liaocheng University in March 2025, and a spherical holly with a diameter of 1.2 to 1.3 m and a height of 0.9 to 1 m was selected for use in the computer-controlled test. The adaptive adjustment of the knife holly pruning machine prototype is shown in Fig. 19. This test used five 12V Chaowei batteries to supply power to all motors, control equipment, *etc*.



Fig. 19. Prototype of holly pruning machine with adaptive tool adjustment

Evaluation Indicators

The pruning leveling rate and branch residue rate were selected as evaluation indexes to visually demonstrate the pruning effect and quality of the holly pruning machine on holly shapes. Each index is the average value of multiple trials, and is defined as follows:

$$P_1 = \frac{Z_1}{Z} \tag{14}$$

In Eq. 14, P_I indicates the percentage of branches and leaves on the whole holly that were leveled and pruned (%), and Z_I indicates the actual number of branches and foliage leveled and pruned by the pruning machine indicates the number of branches and leaves that had to be pruned flat on the whole holly.

$$P_2 = \frac{Z_3}{Z_2} \tag{15}$$

In Eq. 15, P_2 indicates the residual rate of branches and leaves on the whole holly (%), and Z_2 indicates the total number of branches and leaves to be pruned on the whole holly. Indicates the number of branches and leaves that were not completely cut off after pruning the holly pruning machine.

Analytical Methods for Orthogonal Tests

To further optimize the parameters and determine the interactions of the test factors, the ranges of the test factors, such as the pruning mechanism motor speed A, tool tilt angle B, and walking speed C, were determined after careful calculation and analysis. Three-factor and three-level quadratic regression orthogonal tests were carried out using the

pruning leveling rate P_1 and the residual branch residue rate P_2 as the response values. The codes corresponding to each test factor are presented in Table 3.

Table 3. Coding of Test Factors
--

	Factor						
Code value	Trimming Mechanism Motor Speed, A (kr/min)	Tool Tilt Angle, B (°)	Traveling speed, C (m/s)				
-1	9	45	0.8				
0	15	67.5	1.0				
1	21	90	1.2				

The data were analyzed and processed using Design Expert software, and the results of the three-factor, three-level experiment designed according to Box–Behnken's experimental principle are listed in Table 4.

Multiple linear regression and quadratic fitting of pruning leveling rate P_1 and residual branch residue rate P_2 of holly branches and leaves were performed using Design Expert software, and the quadratic regression equations of P_1 and P_2 were derived according to the data shown in Table 4.

$$P_1 = 74.00 + 2.95A - 2.26B - 1.44C + 2.05AB + 0.1000AC + 2.47BC + 2.56A^2 - 1.81B^2 - 3.71C^2$$
(16)

$$P_2 = 11.50 - 0.8000A + 1.58B + 0.8000C - 0.3250AB + 0.2250AC + 0.0750BC - 0.9375A^2 - 1.09B^2 + 1.61C^2$$
 (17)

Table 4. Orthogonal Test Scheme and Test Results

Number		Factor	Response index			
Number	A (kr/min)	B (°) C (m/s)		P ₁ (%)	P ₂ (%)	
1	21	67.5	1.2	75.8	12.7	
2	9	67.5	0.8	70.1	12.1	
3	21	67.5	0.8	75.7	9.7	
4	15	45	1.2	64.2	10.1	
5	9	90	1	66.2	11.4	
6	15	67.5	1	74.1	11.2	
7	15	45	0.8	74.8	9.6	
8	15	67.5	1	74.2	11.1	
9	15	90	1.2	67.1	14.6	
10	21	45	1	79.2	8.2	
11	15	90	0.8	67.8	13.8	
12	9	45	1	77.3	8.8	
13	15	67.5	1	73.8	11.8	
14	15	67.5	1	73.8	11.9	
15	21	90	1	76.3	9.5	
16	9	67.5	1.2	69.8	14.2	
17	15	67.5	1	74.1	11.5	

Analysis of variance (ANOVA) of the regression equations using the Design Expert software yielded Tables 5 and 6. As shown in Table 5, the quadratic regression model (P < 0.05) for the pruning leveling performance of the machine indicated that the regression model was significant. Analysis of variance (ANOVA) indicated that the motor speed of the pruning mechanism (P < 0.05) and tilt angle of the tool (P < 0.05) had a significant effect on the pruning leveling. Analysis of variance (ANOVA) showed that the effects of

the factors on the trimming leveling performance, in descending order of effect, were as follows: trimming mechanism, motor speed, and tool tilt angle. The BC interaction term had a significant effect, proving that there was an interaction between tool tilt angle and walking speed on the trimming leveling. The traveling speed had no significant effect.

Source	Sum of Squares	df	Mean Square	F-Value	<i>P</i> -Value	
Model	265.06	9	29.45	7.41	0.0075	Significant
Trimming mechanism motor speed, A	69.62	1	69.62	17.52	0.0041	
Tool tilt angle, B	40.95	1	40.95	10.31	0.0148	
Traveling speed, C	16.53	1	16.53	4.16	0.0807	
AB	16.81	1	16.81	4.23	0.0787	
AC	0.0400	1	0.0400	0.0101	0.9229	
BC	24.50	1	24.50	6.17	0.0420	
A^2	27.65	1	27.65	6.96	0.0335	
B ²	13.83	1	13.83	3.48	0.1043	
C ²	58.03	1	58.03	14.61	0.0065	

Table 5. ANOVA of the Regression Equation for Pruning Leveling

As shown in Table 6, the quadratic regression model (P < 0.05) for the residue of the holly pruning machine indicated that the regression model was significant. Analysis of variance (ANOVA) showed that the trimming mechanism motor speed (P < 0.05), tool tilt angle (P < 0.05), and walking speed (P < 0.05) had a significant effect on residue retention rate. Analysis of variance (ANOVA) showed that the effect of each factor on residue retention rate, in descending order of effect, was as follows: tool tilt angle, trimming mechanism motor speed, and walking speed.

Table 6.7 (140 V7) of the 100 globalon Equation for 100 state										
Source	Sum of Squares	df	Mean Square	F-Value	<i>P</i> -Value					
Model	49.42	9	5.49	7.08	0.0086	Significant				
Trimming mechanism motor speed, A	5.12	1	5.12	6.60	0.0371					
Tool tilt angle, B	19.85	1	19.85	25.58	0.0015					
Traveling speed, C	5.12	1	5.12	6.60	0.0371					
AB	0.4225	1	0.4225	0.5447	0.4845					
AC	0.2025	1	0.2025	0.2610	0.6251					
BC	0.0225	1	0.0225	0.0290	0.8696					
A^2	3.70	1	3.70	4.77	0.0652					
B ²	4.98	1	4.98	6.42	0.0390					
C ²	10.95	1	10.95	14.11	0.0071					

Table 6. ANOVA of the Regression Equation for Residue

Response Surface Analysis

Using Design Expert software for analysis, the optimized running conditions included a pruning mechanism motor speed of 20.9 kr/min, tool tilt angle of 50°, and walking speed of 0.91 m/s. At this time, the pruning leveling performance was 79.3% and residual branch residue of 8.1% will be now used as the standard value and the response surface in the analysis of the interaction under the change value, to obtain the response surface analysis of the interaction of the factors, as shown in Figs. 20a to 20f.

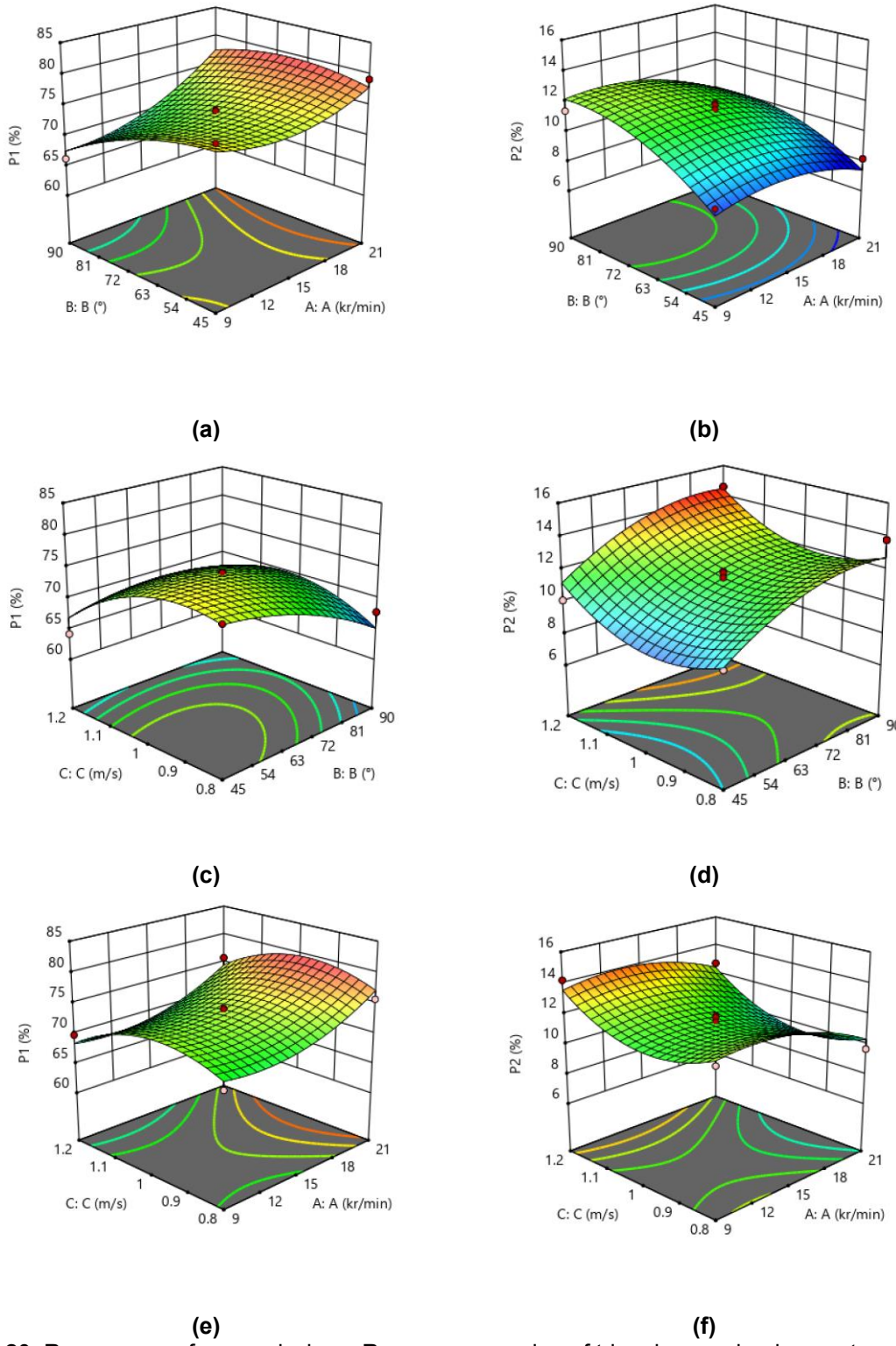


Fig. 20. Response surface analysis: a. Response mapping of trimming mechanism motor speed and tool tilt angle variation with P1 value; b. Response mapping of trimming mechanism motor speed and tool tilt angle variation with P2 value; c. Response mapping of tool tilt angle and travel speed variation with P1 value; d. Response mapping of tool tilt angle and travel speed variation with P2 value; e. Response mapping of trimming mechanism (e) Response maps of motor speed and travel speed with P1 value; (f) Response maps of motor speed and travel speed of trimming mechanism with P2 value

From the response surface analysis above, it can be seen that the change rule of the response surface factors was consistent with the results of the model and the analysis of variance of the regression equation. The results showed that the tool tilt angle B and walking speed C interaction BC had a significant effect on the pruning leveling performance. Finally, the pruning leveling was set to the maximum as the best, and the residue was set to the minimum as the best, through the Design Expert software simulation, simulation to obtain 49 groups of valid data, as shown in Table 7, to determine the two best indicators of holly pruning machine, that is, pruning leveling rate of 79.3% and residue rate of 8.1%.

Table 7. Table of Simulation Results

Number	Α	В	С	P ₁ (%)	P ₂ (%)	Desirability	
1	20.941	50.472	0.914	79.266	8.101	1.000	Selected
2	20.906	50.807	0.934	79.216	8.131	1.000	
3	20.901	50.132	0.911	79.201	8.080	1.000	
4	20.929	50.028	0.927	79.205	8.028	1.000	
5	20.992	49.612	0.931	79.227	7.944	1.000	
6	20.893	50.755	0.914	79.233	8.156	1.000	
7	20.945	51.163	0.915	79.313	8.183	1.000	
8	21.000	48.765	0.904	79.209	7.876	1.000	
9	21.000	48.856	0.921	79.204	7.852	1.000	
10	20.935	51.392	0.941	79.257	8.191	1.000	
11	20.993	51.524	0.960	79.216	8.199	1.000	
12	20.990	50.269	0.902	79.293	8.086	1.000	
13	20.988	51.278	0.956	79.218	8.165	1.000	
14	21.000	48.993	0.923	79.208	7.866	1.000	
15	20.981	51.355	0.953	79.235	8.175	1.000	
16	20.958	49.678	0.925	79.213	7.971	1.000	
17	20.963	49.349	0.918	79.207	7.937	1.000	
18	20.892	50.362	0.921	79.201	8.094	1.000	
19	20.925	50.015	0.921	79.211	8.036	1.000	
20	20.875	50.998	0.928	79.213	8.173	1.000	
21	20.971	50.774	0.948	79.211	8.102	1.000	
22	20.885	50.989	0.920	79.235	8.177	1.000	
23	20.951	50.981	0.911	79.307	8.167	1.000	
24	20.892	51.200	0.934	79.228	8.187	1.000	
25	20.975	49.525	0.917	79.235	7.957	1.000	
26	20.950	51.024	0.948	79.210	8.141	1.000	
27	20.930	50.515	0.918	79.255	8.103	1.000	
28	20.928	50.521	0.896	79.226	8.164	1.000	
29	21.000	51.388	0.961	79.200	8.182	1.000	
30	20.893	50.790	0.904	79.223	8.187	1.000	
31	20.951	50.471	0.888	79.216	8.178	1.000	
32	20.947	50.299	0.925	79.249	8.058	1.000	
33	20.862	50.900	0.912	79.208	8.191	1.000	
34	20.946	50.330	0.903	79.253	8.107	1.000	
35	20.892	50.325	0.916	79.204	8.098	1.000	
36	20.942	51.186	0.939	79.261	8.163	1.000	
37	20.911	50.190	0.922	79.209	8.063	1.000	
38	20.945	51.460	0.949	79.234	8.199	1.000	
39	20.961	50.978	0.899	79.296	8.196	1.000	
40	20.933	51.274	0.947	79.215	8.179	1.000	
41	20.899	50.481	0.910	79.220	8.129	1.000	

42	20.985	51.289	0.931	79.342	8.160	1.000	
43	20.940	50.064	0.902	79.229	8.079	1.000	
44	20.921	50.632	0.922	79.249	8.114	1.000	
45	20.959	49.751	0.893	79.207	8.061	1.000	
46	20.997	51.317	0.958	79.211	8.170	1.000	
47	21.000	49.291	0.870	79.102	8.092	0.997	
48	21.000	46.992	0.889	79.052	7.684	0.995	
49	21.000	47.610	0.935	79.040	7.667	0.995	

CONCLUSIONS

This study independently designed the machine structure and feasibility of a holly pruning machine with adaptive tool adjustment for experimental testing. The kinematics and hydrodynamics simulation analyses of the key components were verified for the design of the key components. The machine will be further improved and tested at a later stage and marketed to promote the development of agricultural and forestry machinery and equipment. The technical innovations and advantages of the machine were studied.

- 1. The lifting mechanism, visual mechanism, walking mechanism, and tool adaptive adjustment mechanism realize the trimming tool position adjustment through synergy, in which the tool adaptive adjustment mechanism adopts multi-degree-of-freedom coupling design, with a large adjustable range, and after the formula derivation and kinetic simulation, it conforms to the principle of rigid-body kinematics, and it can be adapted to the morphology of the holly plant characteristics.
- 2. The control system adopts an industrial-grade PLC as the core processing unit to construct a time-sequence control model. It has a modularized programming architecture, strong anti-interference ability, strong compatibility, powerful logic control ability, and convenient and easy maintenance, which is conducive to improving the efficiency of the entire machine.
- 3. Equipped with the spraying mechanism, holly pruning at the same time can also complete holly pest control work, realizing the dual use of one machine, saving the cost of separate spraying and separate pruning, saving working time, and reducing the waste of manpower and material resources.
- 4. The orthogonal test method is used to determine that the motor rotation speed of the pruning mechanism is 20.9kr/min, and the tool tilt angle is 50°, and the traveling speed is 0.91m/s. At present, the two best indicators of the holly pruning machine were determined to be 79.3% of the pruning leveling rate, and the residual branch retention rate was 8.1%. After field experiments to verify that the above data were accurate, they met the normal working requirements of the machine.

ACKNOWLEDGMENTS

Thank you to the reviewers for their patience and professionalism and for patience with this work.

Funding

This research was funded by Shandong Province Key Research and Development Plan 2019GNC106038 and National College Students Innovation and Entrepreneurship Training Program 202410447012

REFERENCES CITED

- Azlan, Z., Sultan Mahmud, M., Long, H., Heinemann, P., Daeun, C., and Schupp, J. (2021). "Technological advancements towards developing a robotic pruner for apple trees: A review," *Computers and Electronics in Agriculture* 189, article 106383. DOI: 10.1016/j.compag.2021.106383.
- Botterill, T., Paulin, S., Green, R., Williams, S., Lin, J., Saxton, V., Mills, S., Chen, X., and Corbett-Davies, S. (2017). "A robot system for pruning grape vines," *Journal of Field Robotics* 34(6), 1100-1122. DOI: 10.1002/rob.21680.
- Christenhusz, M. J. M., and Fay, M. F. (2024). "The genome sequence of the English holly, *Ilex aquifolium* L. (Aquifoliaceae)," *Wellcome Open Research* 9, 1-1. DOI: 10.12688/wellcomeopenres.20748.1.
- Chen, H., Li, H., Chong, X., Zhou, T., Lu, X., Wang, X., and Zheng, B. (2024). "Transcriptome analysis of the regulatory mechanisms of holly (*Ilex dabieshanensis*) under salt stress conditions," *Plants-Basel* 13(12), article 1638. DOI: 10.3390/plants13121638.
- Chong, X., Wang, X., Zheng, B., Zhou, T., Li, Y., Wang, C., Zhang, F., Zhou, Y., and Chen, H. (2023). "Ning Qing 3: A new holly cultivar with peculiar leaf morphology," *Hortscience* 58(8), 879-880. DOI: 10.21273/hortsci17197-23.
- Feng, L., Zhang, Y., Chen, W., and Mao, B. (2023). "Colletotrichum siamense Strain LVY 9 causing spot anthracnose on winterberry holly in China," Microorganisms 11(4), article 976. DOI: 10.3390/microorganisms11040976.
- Gokavi, N., Mote, K., Jayakumar, M., Raghuramulu, Y., and Surendran, U. (2021). "The effect of modified pruning and planting systems on growth, yield, labour use efficiency and economics of Arabica coffee," *Scientia Horticulturae* 276, article 109764. DOI: 10.1016/j.scienta.2020.109764.
- Guo, Z., Wei, J., Xu, Z., Lin, C., Peng, Y., Wang, Q., Wang, D., Yang, X., and Xu, K.-W. (2023). "HollyGTD: An integrated database for holly (Aquifoliaceae) genome and taxonomy," *Frontiers in Plant Science* 14, article 1220925. DOI: 10.3389/fpls.2023.1220925.
- He, L., and Schupp, J. (2018). "Sensing and automation in pruning of apple trees: A review," *Agronomy* 8(10), article 211.
- Kamandar, M. R., Massah, J., and Jamzad, M. (2022). "Design and evaluation of hedge trimmer robot," *Computers and Electronics in Agriculture* 199, article 107065. DOI: 10.1016/j.compag.2022.107065.
- Kaljaca, D., Vroegindeweij, B., Mencarelli, A., and van Henten, E. (2020). "Coverage trajectory planning for a bush trimming robot arm (vol 37, pg 283, 2020)," *Journal of Field Robotics* 37(6), 283-308. DOI: 10.1002/rob.21917.
- Li, M., Ma, L., Zong, W., Luo, C., Huang, M., and Song, Y. (2021). "Design and experimental evaluation of a form trimming machine for horticultural plants," *Applied Sciences-Basel* 11(5), article 2230. DOI: 10.3390/app11052230.

- Peng, M.-H., Dai, W.-P., Liu, S.-J., Yu, L.-W., Wu, Y.-N., Liu, R., Chen, X.-L., Lai, X.-P., Li, X., Zhao, Z.-X., and Li, G. (2016). "Bioactive glycosides from the roots of *Ilex asprella*," *Pharmaceutical Biology* 54(10), 2127-2134. DOI: 10.3109/13880209.2016.1146779.
- Prasad, M. N. V., and Freitas, H. (2000). "Removal of toxic metals from solution by leaf, stem and root phytomass of *Quercus ilex* L. (holly oak)," *Environmental Pollution* 110(2), 277-283. DOI: 10.1016/s0269-7491(99)00306-1.
- Qiu, L., Sun, J., Zhang, X., Sun, Q., and Zhao, Y. (2024). "A PLC-based pomegranate sprout removal device design," *Scientific Reports* 14(1), article 5137. DOI: 10.1038/s41598-024-55068-8.
- Siktár, B., Kakuk, J., and Hegedűs, G. (2024). "Electromechanical model of a hedge trimmer mechanism," *Multidiszciplináris Tudományok* 14(4), 140-148.
- Su, T., Zhang, M., Shan, Z., Li, X., Zhou, B., Wu, H., and Han, M. (2020). "Comparative survey of morphological variations and plastid genome sequencing reveals phylogenetic divergence between four endemic *Ilex* species," *Forests* 11(9), article 964. DOI: 10.3390/f11090964.
- Thiyagarajan, R. (2024). "Development and performance evaluation of engine-operated bund trimmer," *Asian Journal of Current Research* 9(4), 173-178.
- Westling, F., Underwood, J., and Bryson, M. (2021). "A procedure for automated tree pruning suggestion using LiDAR scans of fruit trees," *Computers and Electronics in Agriculture* 187, article 106274. DOI: 10.1016/j.compag.2021.106274.
- Xu, M. M., Xie, S. N., Li, Y., and Chen, Q. H. (2013). "Structural design of a multi-degree-of-freedom scalable tree trimmer," *Advanced Materials Research* 791, 770-773.
- Zhang, B., Chen, X., Zhang, H., Shen, C., and Fu, W. (2022). "Design and performance test of a jujube pruning manipulator," *Agriculture-Basel* 12(4), article 552. DOI: 10.3390/agriculture12040552.
- Zhou, P., Zhang, Q., Li, F., Huang, J., and Zhang, M. (2023). "Assembly and comparative analysis of the complete mitochondrial genome of *Ilex metabaptista* (Aquifoliaceae), a Chinese endemic species with a narrow distribution," *BMC Plant Biology* 23(1). 393. DOI: 10.1186/s12870-023-04377-7.
- Zhou, T., Zhou, Y., Wang, C., Li, Y., Zhang, D., and Chen, H. (2023). "Ning Qing 1: A new holly cultivar with broadly ovate leaf morphology," *HortScience* 58(12), 1626-1627. DOI: 10.21273/hortsci17413-23.
- Zhou, T., Chong, X., Zhang, F., Lu, X., Zhang, D., and Chen, H. (2024). "Ning Qing 4: A new holly cultivar with elliptic and serrated leaves," *HortScience* 59(1), 16-17. DOI: 10.21273/hortsci17436-23.

Article submitted: April 27, 2025; Peer review completed: May 18, 2025; Revised version received: May 26, 2025; Further revised version received and accepted: June 18; Published: June 25, 2025.

DOI: 10.15376/biores.20.3.6736-6764